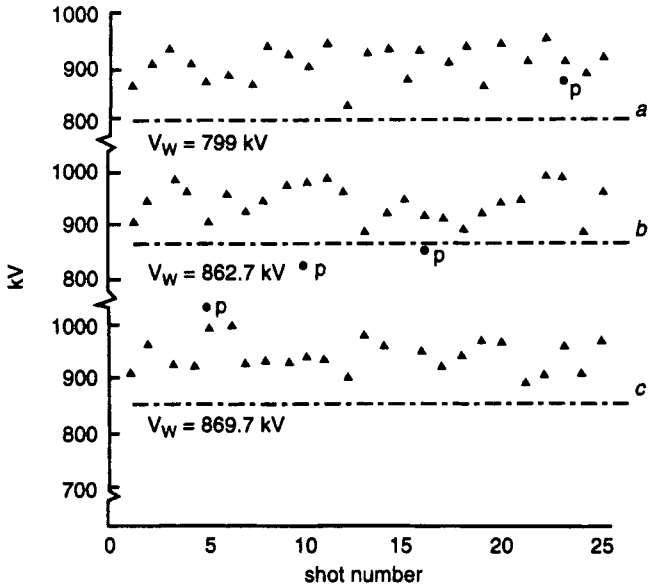

Figure 3.18 *Sequence of 50 Hz breakdown levels in SF_6 for perturbed electrode system F (SF_6 pressure: 0.2 MPa)*
– – – – *V_{TH} Theoretical breakdown level (1148 kV)*
* *(based on $(E/p)_{lim}$ = 89 kV mm^{-1} MPa^{-1}*
▲ *individual spark breakdown*
*p *'PIP' – partial (incomplete) breakdown*
V_w *maximum (1 min) withstand level, established immediately prior to test runs a, b or c, respectively*

corresponding 60 s highest withstand levels (V_w) are also given. Some salient findings emerge:

1. Figure 3.16, curves (a), (b) and (c), relate to a 50 Hz voltage test sequence for three 'successive' test series for a concentric cylindrical electrode system.

   - Curve (a) illustrates that whereas the highest '60 s withstand level' V_W was 480.8 kV_{pk}, the sequence of 'twenty-five instantaneous' breakdown levels was significantly higher, being within the range 520–595 kV_{pk}. For the purposes of comparison, the theoretical critical breakdown voltage level (V_{TH}) is 621.6 kV_{pk}, based on a critical $(E/p)_{lim}$ = 89 kVmm^{-1} MPa^{-1}.
   - Curves (b) and (c) show corresponding results for two repeat series. Here, it can be seen that the corresponding '60 s withstand' levels (V_W) increased significantly to 565.7 and 594 kV_{pk}, respectively, as compared to the level of 480.8 kV_{pk} obtainable in the first test series, i.e. curve (a).

- Similarly, it can be seen from the sequence of individual 'instantaneous breakdown' levels (V_b) that, despite occasional low level breakdowns, a significant 'conditioning' effect has taken place and, in curve (c), approximately 10 of the 25 'instantaneous breakdown' levels achieved breakdown values of $\approx$600 kV_{pk}, i.e. within 3.5% of the theoretical limiting breakdown level.

2. Figure 3.17 shows comparable 50 Hz results for a perturbed concentric cylinder electrode system (F). As before, the results presented in curves (a), (b) and (c), respectively, relate to three complete test series. Once again, the sequence of 'instantaneous breakdown' results exhibit a noticeable voltage 'conditioning' effect, with occasional low level results, e.g. curve (c), the conditioned level of $\approx$590 kV_{pk} being within 3% of the theoretical breakdown value. Returning briefly to the sequence of highest '60 s withstand' levels for the test series (a), (b) and (c) (Figure 3.17), it is noted that V_w increases as the test series proceeds, corresponding values being 509.1, 544.5 and 558.6 kV_{pk}, respectively.
3. Figure 3.18 provides comparable results, obtained at higher SF_6 gas pressures. Under these conditions, 'instantaneous breakdown' values were significantly lower than corresponding theoretical levels, e.g. being lower at 0.2 MPa, by between 15 and 31%, for this electrode arrangement.
4. Figure 3.19 shows some further results for a larger concentric cylinder electrode system (I), [see Table 3.3], which illustrate similar trends at 0.1 MPa but show a very significant spread in the SF_6 'instantaneous breakdown' levels as compared to the '60 s withstand' level (V_w) of 795 kV_{RMS}, at the higher gas pressure 0.45 MPa [see curves (d), (e) and (a)]. Here, the values of V_w tend to be lower than the theoretical limiting levels V_{TH} by between 18 and 60%, the difference increasing with SF_6 pressure. It should also be noted [curve (a)], that the lowest recorded breakdown level corresponds to a stress figure of $\approx$ 8 kV_{RMS}/mm, significantly higher than the working stresses for GIS equipment referred to earlier.

Extensive data exists for SF_6 gas-gaps under clean and contaminated conditions (see References 13, 23–28, for example). It is now established that the presence of particulate contamination of lengths 2–20 mm can reduce the dielectric withstand capabilities of practical gaps by varying amounts up to typically 30, 40 and 70% for lightning impulse, switching impulse and power frequency conditions, respectively, at working SF_6 pressure. Figure 3.20 illustrates a typical spread in 50 Hz flashover levels for varying degrees of gross contamination and represents the maximum lowering of withstand that can be expected [13].

Barrier performance data: Careful design and assembly of the cast

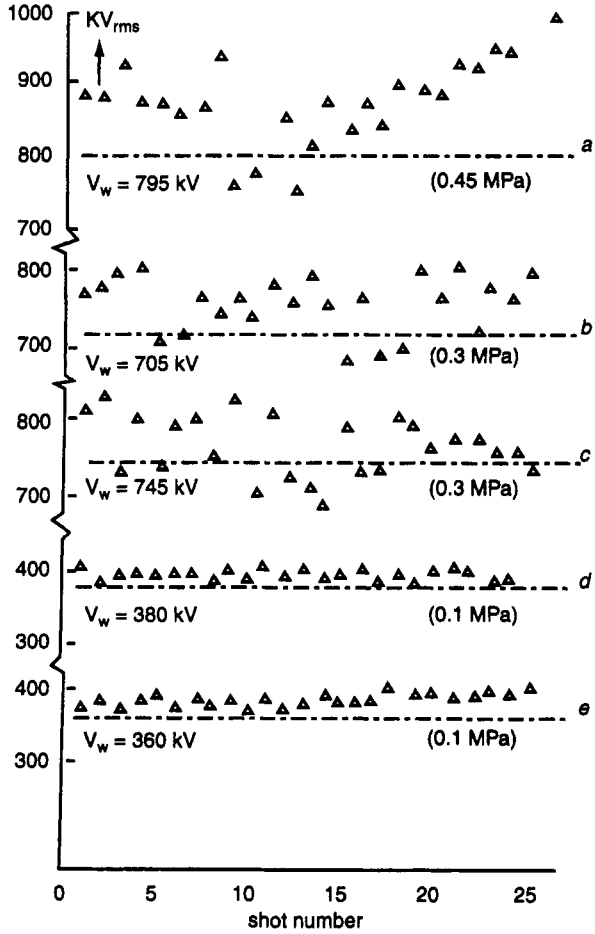

Figure 3.19 *Sequence of 50 Hz breakdown levels in SF_6 for large concentric cylinders (Electrode system I, SF_6 pressure: 0.1–0.45 MPa)*
△ *individual spark breakdown*
V_w *maximum (1 min) withstand level, established immediately prior to test run*

resin support barriers used in SF_6 insulated GIS equipment is vitally important. It should be noted that, for a particular gas pressure, the withstand characteristics of support barriers in SF_6 under clean conditions depends on the particular resin formulation used, the insulation shape and on the disposition of stress relieving fitting, insert, etc. Typical withstand gradient levels of 11.6, 8.7 and 6.6 kV_{pk}/mm can be achieved under lightning, switching impulse and 50 Hz short term voltage conditions, respectively [13].

The presence of particulate contamination can reduce the 50 Hz

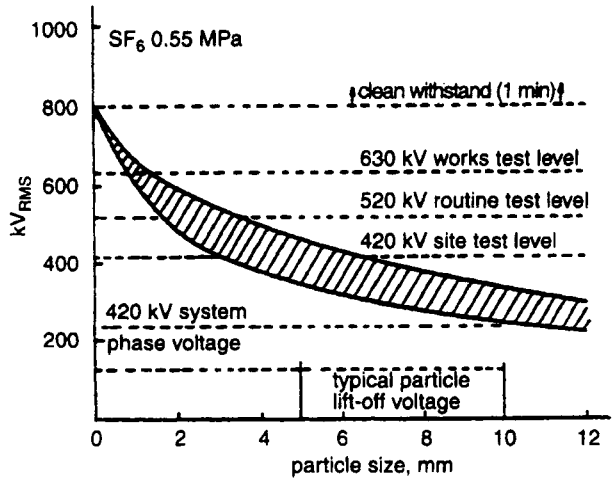

Figure 3.20 50 Hz flashover characteristics of epoxy resin conical spacers under varying degrees of metallic contamination [10]

withstand capability of cast-resin support barriers in SF_6 gas by varying amounts (e.g. up to < 30%) depending on particulate size and disposition. For the most onerous dispositions of cast-resin support barriers, the percentage lowering of 'withstand' performance under impulse conditions tends to be much less than that experienced for 50 Hz test conditions, for comparable levels of contamination (see Figures 3.20 and 3.21, for example) at spacer gas gap interfaces. The reader should compare these findings for 100% SF_6 with Figure 3. 11, diagrams e–g, relating to particle initiated breakdown in SF_6/N_2 mixtures. These workers [29] consider that particle initiated breakdown is more complicated in SF_6/N_2 mixed gas than in 100% SF_6 gas and they recommend that further studies are necessary to achieve a better understanding of the discharge mechanisms.

3.4.3.2 GIS equipment: power frequency (V/t) characteristics

An understanding of voltage gradients that can be safely sustained in service in GIS emerges from extensive laboratory studies, relating specifically to long-time 50 Hz test conditions. The ratio *E/p* is a convenient measure of the stress applied to GIS equipment in service. Typical normalised working stress/gas pressure ratios (*E/p*) are 7 MV/MPa and 3 MV/MPa for SF_6 insulated switchgear including instrument transformers, for 300 and 420 kV systems [4, 13], are shown in Figure 3.22. This figure was originally prepared in 1983, at which time many of these units had been in service for periods up to 15 years and excellent service reliability had been demonstrated. It should be noted that this equipment

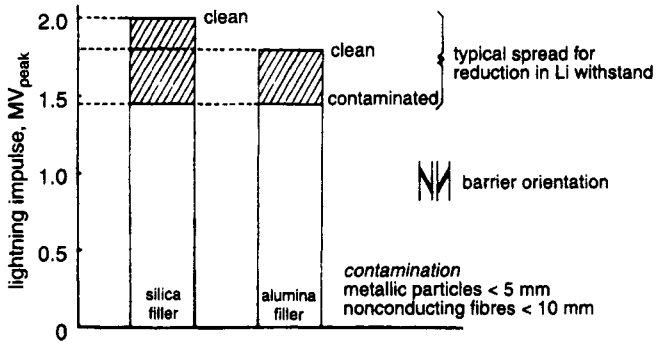

Figure 3.21 Limit of lightning impulse withstand capabilities of epoxy resin conical spacers under clean and contaminated conditions

continues to provide excellent service reliability, some 30 + years after going into service [13]!

It is readily apparent (see Figure 3.22) that the maximum service stress levels for gas-gaps in SF_6 insulated switchgear are relatively low, i.e. < 4 kV_{RMS}/mm, when compared to the significantly higher attainable withstand characteristics achievable (see curves, Figure 3.15). The working stress levels shown in Figure 3.22 can be considered to be generally representative of modern GIS installations. By restricting these gradient levels well below the limiting values, deduced from long-term laboratory studies, manufacturers ensure the long-term dielectric integrity of their equipment – provided, of course, that the normal rigorous quality control and in-service condition monitoring procedures have been maintained.

The importance of component cleanliness, achieved during factory construction, testing, site assembly and commissioning of GIS, and subsequently throughout the entire service life of SF_6 insulated equipment, is now fully appreciated worldwide. Cleanliness, linked with good design, assembly and the introduction of sophisticated 'in-service condition monitoring' practices are recognised as being vitally important factors to resolve if safe and reliable operation is to be achieved throughout the service lifetime of GIS, which should exceed > 40 years. In recent years there has been much progress in the development of effective UHF condition monitoring techniques [30–32]. These strategic developments are considered further in several of the later chapters.

Critical areas of metalclad designs have been identified which merit special manufacturing, testing and assembly controls, and these aspects will be further considered in Section 3.5 and also in later chapters. Several papers have considered the power frequency (V/t) characteristics of gaseous and solid insulation using model gas-gaps and gas/insulator

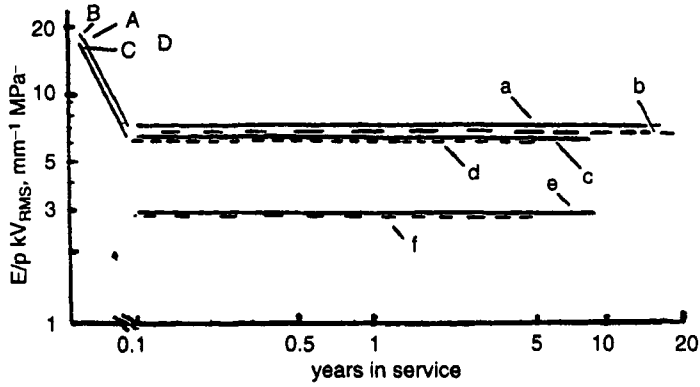

Figure 3.22 *Normalised 50 Hz service E/p levels for SF_6 insulated switchgear equipment*

a, A	*420 kV post-type current transformers*
b, B	*300 kV post-type current transformers*
e, c, C	*300 kV GIS equipment*
f, d, D	*420 kV GIS equipment*
a, b, c, d, e	*service stress levels*
A, B, C, D	*factory 50 Hz 1 min test level at working pressure*

Working pressure:

a, A	*0.38 MPa*
b, B	*0.38 MPa*
c, C	*0.40 MPa*
d, D	*0.55 MPa*

arrangement for large electrode systems under conditions with 'gross' contamination present and with varying gas pressures [13].

3.4.4 Performance under contaminated conditions

As has been demonstrated above, the achievable design stress and reliability of SF_6 insulated apparatus under normal power frequency service conditions is crucially affected by particulate contamination. Particles in the gas space and on the insulator surface can significantly lower the dielectric strength of the system. In SF_6, the breakdown voltage for a relatively long particle, fixed in contact with the conductor, is considerably higher than that for a number of free conducting particles, over a limited range of pressures. Under power-frequency voltage excitation, free conducting particles tend to bounce along the bottom of the enclosure or across the surface of the insulators. The amplitude of individual bounces depends on the particle size and shape, the potential on the system and other random parameters. Particle initiated breakdown can occur at voltages considerably lower than those required for breakdown due to the roughness of the electrode surfaces and is, in general,

lower for negative impulse polarity voltages [26]. Since then, switchgear and CGIT manufacturers – in support of GIS and GIL equipment developments – have undertaken comprehensive evaluation of the dielectric performance characteristics of practical gas-gap arrangements and solid support insulation configurations in SF_6, under both clean and contaminated conditions. Such studies can involve comprehensive laboratory tests to determine, and quantify, the effects of particulate contamination size on the breakdown voltage in SF_6, under conditions representative of both gas insulated 'backparts', circuit-breakers, disconnect switches, etc. and for GIL configurations, for widely varying experimental conditions.

Numerous interrelated factors can influence the degree to which the presence of particles can lower the the dielectric 'withstand capabilities' of GIS under normal service conditions. These depend on:

- length and diameter of particles present
- whether particles are metallic or nonmetallic
- quantity and nature of contamimant material (density, etc.)
- position of particles relative to electric field and also to various GIS components
- actual design and physical disposition of GIS components (e.g. whether circuit-breaker, backparts, etc. are mounted horizontally or vertically)
- type of particle movement, when electrostatic forces exceed those of gravity
- working gas pressure of SF_6 or gas mixtures
- effectiveness of particle 'collection' or 'trapping' techniques.

The above factors are now well known and appropriate procedures are implemented to avoid any problems (see Section 3.4.3.2 above). Manufacturers and utilities take immense care in the design, testing, site-commissioning and also the ongoing 'in-service performance monitoring of GIS' throughout the lifetime of the equipment. At the outset, for a user to be able to decide on what GIS, 'data' are needed on which to judge investment and maintenance decisions. To cover these strategic aspects, very high frequency, UHF, condition monitoring techniques have been developed and installed in many GIS installations wordwide [30–32]. Currently, the need, justification, design, dependability, management of information, and future application of monitoring and diagnostic techniques are under critical review by CIGRE [32].

3.4.5 GIS service reliability

A recently issued report [33], briefly outlining the findings of a second major CIGRE survey, states that GIS technology has contributed very

effectively to increasing the reliability of new substations and to improving the asset life-cycle of existing ones. This extensive study on high voltage substations provides a database of GIS service experience survey on SF_6 insulated equipment, covering collected information referring to more than 13 500 circuit-breaker bays and 118 500 bay years. The survey presents a valuable history, providing an analysis of results on installation and GIS major failure reports data, including:

(a) general data about GIS installations
(b) data concerning GIS failure frequencies
    (i) Failure frequency overview, trend of major failure frequency during the GIS lifetime
    (ii) failure frequency-comparison with 1st CIGRE, GIS survey
(c) major failure characteristics
    (i) basic characteristic data overvoltage classes (identification of main component, or GIS part involved in the failure, identification of sub-assembly or component responsible for the failure
    (ii) classification of symptoms, cause of the failure, service circumstances, operational circumstances
    (iii) type of repair, immediate consequences of the failure, characteristics of the repair, correlation between basic characteristic failure data.

Also considered in this survey were life expectancy, maintenance and environmental issues:

(a) life expectancy
    (i) for already installed GIS
    (ii) for newly installed GIS
(b) maintenance practice
    (i) routine preventive maintenance
    (ii) major preventive maintenance
(c) extension and uprating
(d) environmental issues
    (i) SF_6 handling
    (ii) SF_6 leakage rates
    (iii) analysis of failure relating to SF_6 gas
(e) electromagnetic phenomena.

It is hoped that the data presented [33] will provide a valuable resource and benchmark for both users and manufacturers operating within the field of GIS substation planning, design, construction and service. This

is undoubtedly a valuable document for anyone interested in the application of gaseous insulation. Nevertheless, it must be recognised that the document has certain shortcomings, due to commercial and statistical constraints, which prevents one obtaining a totally 'holistic understanding' of all failure patterns, etc.

3.4.6 Vacuum switches

Vacuum, at better than 10 torr, has an electric strength of typically 30 kV/mm; under arcing conditions, gas for ionisation is provided by molten metal at the arc root of the electrodes and vacuum breakdown is very dependent on electrode conditions. Arc interruption in vacuum circuit-breakers (VCBs) is therefore achieved (Reece [2]) by cooling the arc root quickly to suppress the hot spot. This is achieved by rotating the arc root rapidly under its own magnetic field and by using electrode materials of high boiling point and good thermal conductivity. The high electric strength of vacuum ensures that once the arc is suppressed, usually at the first current zero, no re-ignition occurs and dielectric recovery is achieved within a few μs.

The contacts are housed in a sealed glass or ceramic bottle (Figure 3.23) with a moving metal bellows and are maintenance-free. Excellent service performance has been demonstrated for fault currents of <40 kA and 33 kV operation. VCB are ideal for use where many breaker operations are required, for example in railways and arc-furnaces. The impulse level (150 kV) on the small gap (10 mm) limits the working voltage of a single bottle, but bottles have been stacked in series to provide 32 kV breakers (Reece [2]). The major use of VCBs is in 11, 33 or 66 kV applications for distribution use where an 'oil-free', 'maintenance-free', breaker is required. Typical applications of VCBs and SF_6 interrupters are discussed further by Pryor and Ali in Chapters 10 and 11, respectively, of this book.

3.5 System modelling

3.5.1 Field analysis techniques

The electrostatic fields of high voltage equipment are satisfied by the well known Laplacian equation which takes the form

$$\nabla^2\varphi = \frac{\partial^2\varphi}{\partial x^2} + \frac{\partial^2\varphi}{\partial y^2} + \frac{\partial^2\varphi}{\partial z^2} = 0$$

where φ is the potential at any point in the Cartesian co-ordinate system x, y, z. The field distribution in any design is dependent on the shape, size

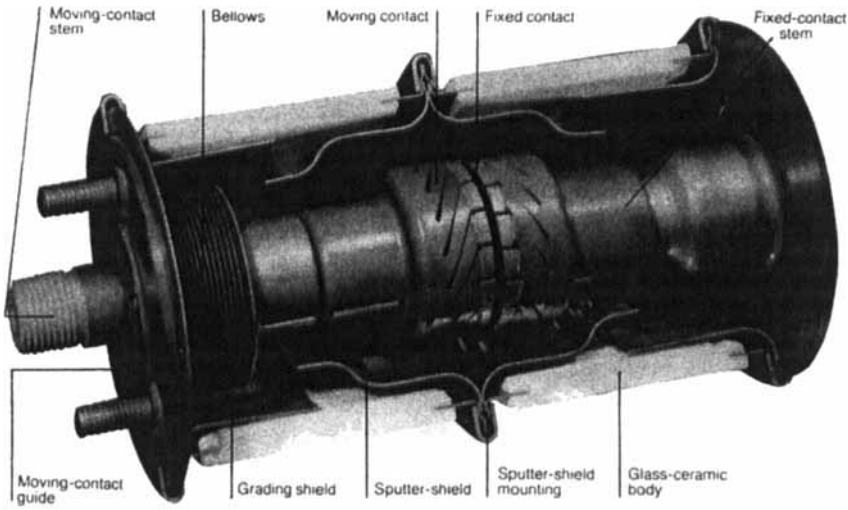

Figure 3.23 Section view of vacuum interrupter (Courtesy Vacuum Interrupters Ltd and [4, Chap. 6])

and disposition of the electrodes and insulation and also, in general, on the permittivities of the insulating materials used.

One criterion which can be applied to the evaluation of the electrostatic design of high voltage equipment is the ratio of the average to maximum field. This parameter, termed the utilisation factor η, is considered below, together with details of a related parameter termed the normalised effective electrode separation. Brief reference is made in Section 3.5.1.3 to a simple approximate two-dimensional method which can often be used to estimate maximum voltage gradients for complicated arrangements which cannot be solved directly by available numerical methods.

Analytical solutions of the Laplace equation can only be obtained for relatively simple electrode systems, where the conducting surfaces (electrodes) are cylinders, spheres, spheroids or other surfaces conforming to equipotentials surrounding some simple charge distribution. Generally, the multiplicity of boundary conditions for the complicated contours encountered in high voltage equipment means that analytical solutions of the potential are not possible. Because of this difficulty, several approximation methods have been investigated, the more important of these being (i) analogue methods and (ii) numerical methods [21, 34].

3.5.1.1 Utilisation factor approach

In the evaluation of the electrostatic design of high voltage equipment, an important consideration is the effectiveness with which the available

space has been used. For the region which encompasses the minimum distance between conductors, the ratio of average to maximum electric stress (E_{av}/E_{max}) is a useful criterion. This ratio, termed the utilisation factor η, measures the inferiority of the field system in comparison with that between infinite plane parallel electrodes [35], where $\eta = 1$. In the literature, the reciprocal term $1/\eta$ called the field factor (f) is sometimes preferred. Tables of η exist [35,36] for several standard electrode systems for wide ranges of so-called geometric characteristics p and q, where $p = (r + g)/r$ and $q = R/r$. Subscripts 2 and 3, respectively, are used to denote two- and three-dimensional systems. Appropriate formulas are given elsewhere, use being made of existing solutions of Laplace's equations [34–41]. These calculations assume constant permittivity but techniques can be extended to multi-dielectric problems.

Some calculated values of η are also presented in graphical form in Figure 3.24. It is immediately evident that η for each geometry tends to decrease as the geometric characteristic $p = (r + g)/r$ increases. This can

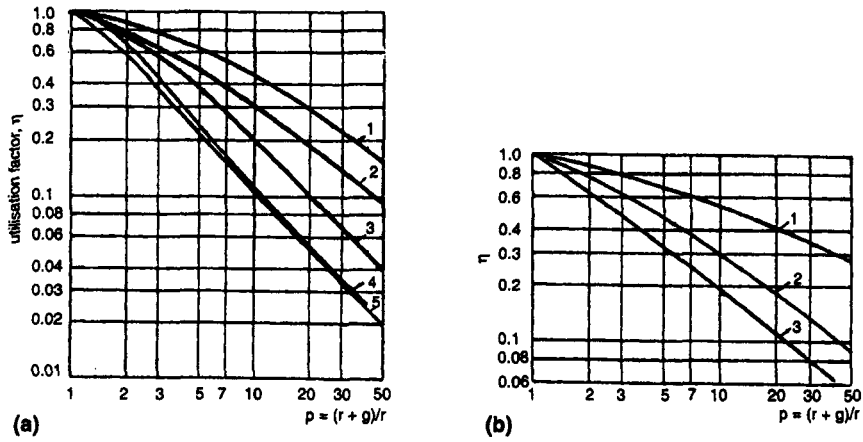

Figure 3.24 *Dependence of η upon geometric characteristic p for a few simple geometries*

(a) *Curves 1 cylinder–cylinder*
2 cylinder–plane
3 sphere–sphere (symmetrical supply)
4 sphere–sphere (unsymmetrical supply)
5 sphere–plane

(b) *Curves 1 hyperbolic cylinder*
2 hyperboloid (points)
3 hyperboloid (point)–plane

be explained by the increased divergence of the field as p increases. Furthermore, it is noted that, for a particular value p, η for a three-dimensional geometry is lower than that for the corresponding two-dimensional geometry (e.g. compare cylinder-plane and sphere-plane, curves 2 and 5, Figure 3.24). Once again, this may be attributed to the greater field divergence in the three-dimensional arrangements. Brief mention will be made later to the simple relationship existing between η for corresponding two- and three-dimensional systems. To summarise, utilisation factors, or field factors, may be calculated for many practical arrangements either as a result of precise analysis for simple geometries or, for more difficult configurations, by approximate numerical or analogue techniques together with appropriate difference equations discussed elsewhere [36].

3.5.1.2 Efficiency factor concept

For certain design problems, conditions of fixed axial distance must be complied with. The utilisation factor has the limitation that it does not take into account the space necessary to accommodate the electrode geometry. To allow for this, η can be multiplied by the electrode separation g. The product of these terms gives the 'effective electrode separation' α of the system. If, now, α is divided by some measure of the total dimension available, a new quantity λ is obtained, which is really the normalised effective electrode separation of the system. The efficiency factor concept (λ) is sometimes useful when designing high voltage equipment, particularly when conditions of fixed axial distance d exist [35]. For a particular operating voltage V it is possible to keep the maximum stress at the electrode surface to a minimum by selecting the best size, shape and disposition of electrodes for conditions of constant d (see Figure 3.25). Under these conditions $\lambda = \hat{\lambda}$ and $E_m = V/\hat{\lambda}d$.

All the results referred to above assume a single value for the dielectric constant. If two or more dielectrics are being considered, then the concepts of utilisation factor and efficiency factor could be applied to each dielectric separately. These techniques have been widely used to assist in electrostatic aspects of GIS design for many years.

3.5.1.3 Approximate two/three-dimensional concept

The electrode arrangements considered above contained at least one axis of symmetry. In many practical arrangements, however, such symmetry does not exist. In the absence of symmetry, the problem of making accurate pronouncements on maximum field strengths for practical three-dimensional systems often becomes complicated since it is sometimes either exceedingly difficult or even impossible to make single

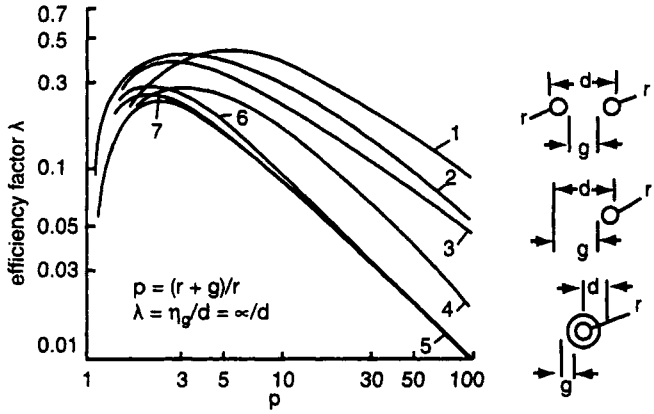

Figure 3.25 *Dependenced of λ upon p for several standard geometries*
Curve 1 parallel cylinders; curve 2 cylinder–plane; curve 3 concentric cylinders; curve 4 sphere–sphere (symmetrical supply); curve 5 sphere–sphere (unsymmetrical supply); curve 6 sphere–plane; curve 7 concentric spheres

realistic numerical or analogue model representation without introducing appreciable errors.

It would be useful if, for example, one could obtain even an approximate solution for a particular practical three-dimensional representations (having conductors similar to axial and radial sections of the original three-dimensional conducting surfaces), which, in general, can be more easily solved. Boag and later Galloway *et al.* [34] investigated the possibilities of this simple approach and have analysed numerous simple configurations. Ryan has produced useful correction curves (see Figure 3.26), which can be used with acceptable accuracy.

3.5.1.4 Numerical methods

Numerical methods of solution, which express the Laplacian equation in finite terms, provide a powerful means of calculating the electric fields of practical arrangements. A great deal of published literature exists relating to this subject. For a useful background overview of this sector, the reader should refer to the technical literature, which contains many useful practical applications of the numerical modelling techniques now readily available to support gaseous/solid/liquid insulation studies, covering electrostatic, electro-magnetic, thermal and arc interruption modelling and equipment design. A few sources are given as follows:

1. In contrast to other workers who have used relaxation techniques Ryan and colleagues [34, 37, 41] developed a computer program to solve

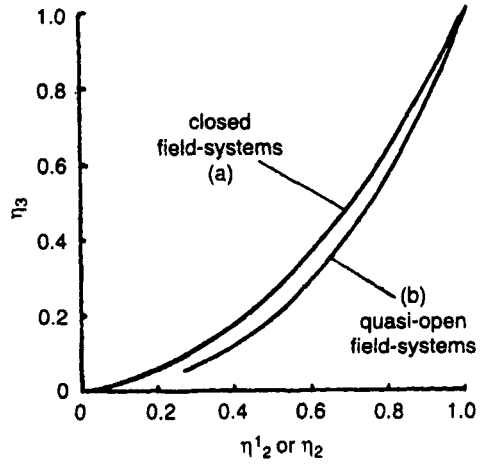

Figure 3.26 Correction curves [37]
(a) Applies for
concentric cylinders and concentric spheres
cylinder–plane and sphere–plane
hyperbolic cylinder–plane and hyperboloid plane
parabolic cylinders and paraboloids of revolution
(b) Applies for systems shown in Figure 3.25

the Laplace equation in two dimensions and three dimensions with one axis of symmetry by an exact noniterative method. This method was selected after various techniques for solving the resultant set of simultaneous equations had been studied. The main details of this program, together with numerous illustrations of its extensive application in support of switchgear design are given in References 34 and 41. Two important examples of such work are shown in Figures 3.27 and 3.28 will be considered in the next two sections.

2. Binns and Randall [42] have described an overrelaxation method and give details of various accelerated finite difference formulas used. In this investigation, potential gradients were calculated around a spherical high voltage electrode separated from an earthed plane of a recessed dielectric slab. The potential gradient transitions were determined and analysed at the point where the surface of the recessed dielectric slab meets the sphere surface.

3. Storey and Billings [43] have described a successive over-relaxation method suitable for determining axially symmetric field distributions. They also discuss a method for the determination of the three-dimensional electric field distribution in a curved bushing.

4. The ISH Symposia series (International symposium on *High voltage engineering*) provides an excellent resource to keep abreast of the latest work in the HV sector, including numerical field techniques. This

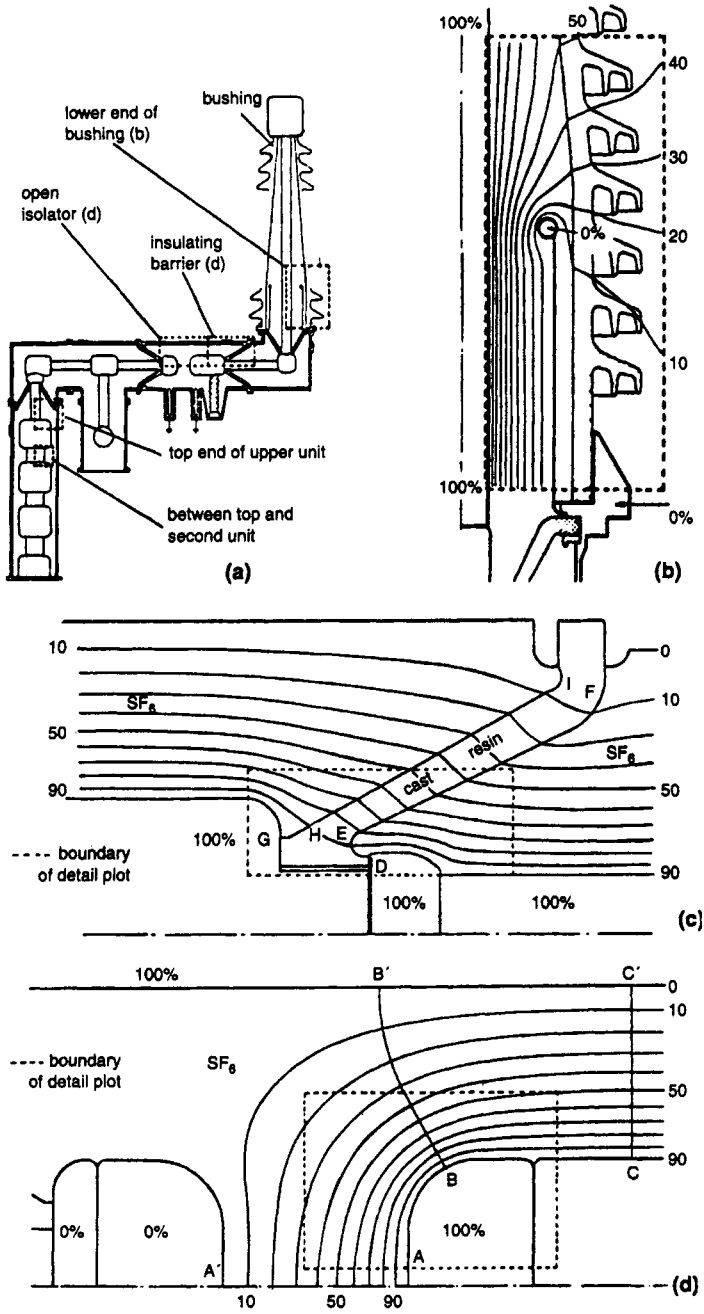

Figure 3.27 *Computer field study of an early 300 kV metal-clad switchgear design [21]*
(a) *Part of single phase layout;* **(b)** *field plot at lower end of bushing;* **(c)** *field plot of barrier supporting isolator;* **(d)** *field plot in vicinity of open isolator*

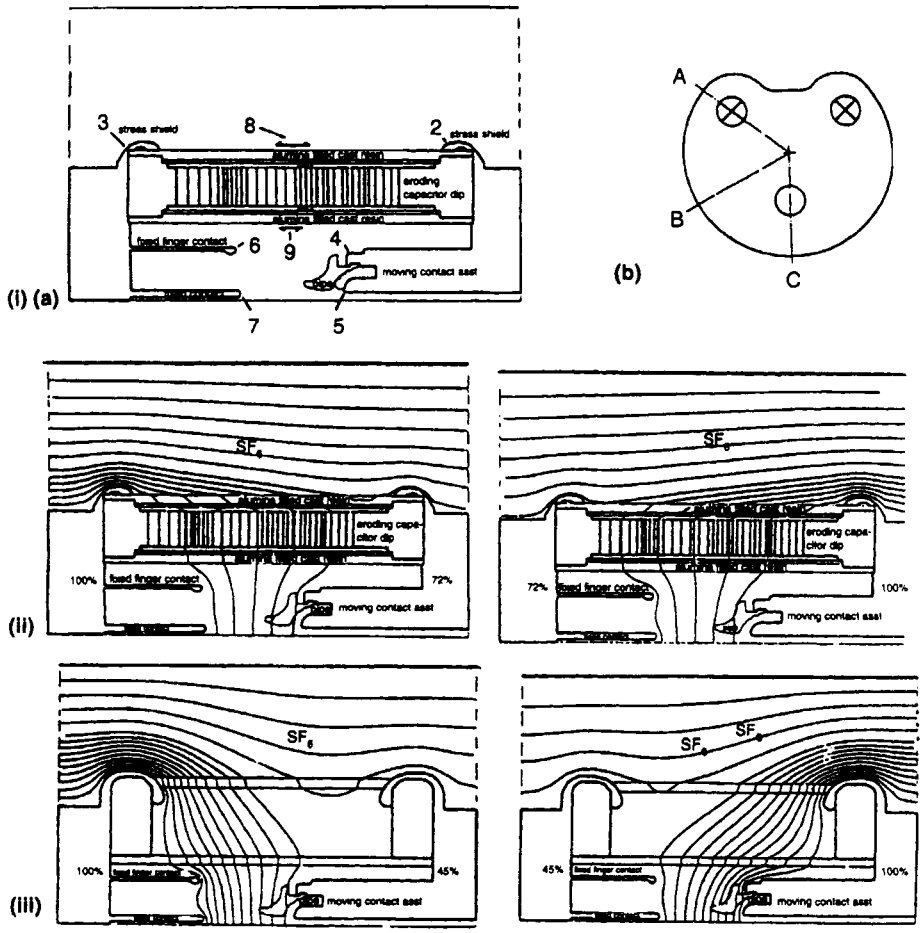

Figure 3.28 *E-field design studies relating to the development of heavy duty SF_6 interrupters in the 1980s [21]*

- **(i)** *Identification of regions of interest: (a) general location of regions 2–9; (b) plan view, illustrating three radial sections, A, B and C*
- **(ii)** *Typical E-field plots: first interrupter of 4-break design; through capacitor (section A)*
- **(iii)** *Typical E-field plots: first interrupter of 2-break design; through empty support tube (section B)*

symposia series has been held at regular intervals over more than 27 years: Munich (1972), Zurich (1975), Athens (1983), Braunsweig (1987), New Orleans (1989), Dresden (1991), Yokohama (1993), Gratz (1995), Montreal (1997), London (1999) and Bangalore (2001).

Since the work [34,37,41] was carried out, much valuable information has appeared in the literature regarding finite element, finite difference,

boundary integral and other variants. Numerous commercial field analysis packages are now available. Indeed, further examples are presented in later chapters. A detailed discussion of relaxation methods, difference formulas, accelerating factors, etc. is outside the scope of this chapter. A strategic message from this writer is that, whatever package is to be used, care should be exercised to confirm its effectiveness, and the achievable accuracy, by means of simple validation studies. Once this has been demonstrated and carefully verified, the techniques successfully used by Ryan and others can be adopted with confidence.

3.5.1.5 GIS backparts and insulating spacer design

With the widespread interest in gas insulated cables, busbars, etc., considerable attention has been given to the design of spacer shapes for such equipment. The examples summarised in Figure 3.27 illustrate the extensive use made of analytical field techniques, during early insulation development work on a EHV, SF_6 insulated metal-clad switchgear installation [21].

3.5.1.6 GIS interrupter design

In the 1980s, the trend with GIS equipment was towards more compact designs and interrupters with fewer breaks per phase. As a consequence, the dielectric design and performance of SF_6 circuit-breakers became more critical. Careful shaping of stress shields, optimisation of stress in gas-gaps and the careful selection and profiling of insulation materials, including support insulation (e.g. spacers/barriers) were required. All these and other aspects were thoroughly considered at the design stage, using available software tools, e.g. computer field analysis programs, which had been carefully developed, verified and used extensively to study, critically analyse and optimise, design stresses in GIS and other switchgear designs, for over 35 years [14, 34, 41]. Earlier papers have described field studies during the sequential development of 4-, 2- and 1-break, heavy duty, high performance SF_6 puffer circuit-breakers, for voltages up to the highest system ratings (see [21]). Figure 3.28 shows typical field plots for 4- and 2-break designs. Briefly, after extensive field studies, closely linked with HV and high power development testing for a 4-break design, it was possible to critically analyse all results, before 'sequentially' repeating the exercise for 2-break design and later for a 1-break design. However, the vital difference was that the extensive database gathered, prior to and during development of the 4-break interrupter design, enabled the dimensions, profiles, etc. for the 2-break, and subsequently a 1-break, design to be carefully, and indeed appropriately, selected prior to costly testing. Indeed, it could be argued that this successful development represented a good example of 'rapid-prototyping' or even 'vitual-prototyping' [21]. In any event, it is hoped that this brief

example provides the reader with evidence of the strategic use, with significant savings regarding product development time and cost, that can be gained from the effective use of available 'design databases' together with analytical tools, such as the field analysis modelling techniques referred to in this chapter.

3.5.2 Prediction of breakdown voltages

3.5.2.1 Empirical approach

In 1961, Ryan first investigated the feasibility of using simple estimation methods of predicting the minimum breakdown voltage levels of nonuniform field configurations in gas insulated equipment.

Initially, the method suggested by Schwaiger was considered and later extended [35–41] to more complex electrode configurations by incorporating simple perturbation principles. The method does not consider breakdown mechanisms but is based on a simple discharge-law concept [40].

By ignoring space charge effects, the breakdown voltage V is given by the relationship

$$V_s = E\eta g \tag{3.1}$$

where E and g are the appropriate breakdown gradient and gap dimension, respectively, and η, derived from Laplacian field analysis, is the utilisation factor (ratio of average to maximum voltage gradient (E_{av}/E_m). Initially, standard electrode geometries amenable to precise electrostatic field solution were considered, and extensive tabulated field data has been published [35, 36]. Results of early investigations (e.g. Figure 3.29) firmly established the usefulness of this simple concept for estimating minimum breakdown voltage levels.

In the past, the only major limitation to the application of this empirical approach to switchgear insulation design evaluation has been the lack of reliable breakdown information. Ryan and colleague have made significant contributions [25, 39] in this area and have shown that critical breakdown gradients (E_{50}) and highest withstand gradients (E_w) in air and SF_6 can be accurately represented by relationships of the form

$$rE = K_1 pr + K_2 \tag{3.2}$$

where K_1 and K_2 are constants, $p = [(r + g)/r]$ and r is the radius of the inner cylinder or sphere. The real virtue of this simple empirical breakdown estimation technique is the fact that one can often consider practical electrode systems to be perturbations of the same simple geometry [37].

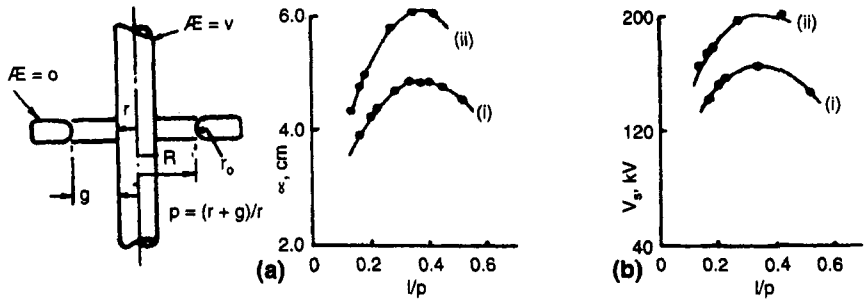

Figure 3.29 *Dependence of α and 50 Hz V_S on l/p for conductor and earthed plate electrode system in air at STP [40]*
(a) *Electrostatic field study (α = ng)*
(b) *High voltage study:*
(i) R = 4.5 in, r_o = 1.0 in (using a range of values of conductor r)
(ii) R = 5.5 in, r_o = 1.0 in (using a range of values of conductor r)
– – – – predicted $V_s = E_s ng$, where $E_s = 27.2 + 13.35\sqrt{r}$ (kV/cm)] and r, g is in centimetres
o experimental

The simple electrode system shown in Figure 3.29 provides a good example to illustrate the effectiveness of this simple empirical breakdown estimation technique. An estimate of the anticipated breakdown voltage characteristics of this arrangement (Figure 3.29) is required, in atmospheric air under standard conditions [$T = 20$ °C, $P = 760$ mm]. We can consider this electrode system to be a 'perturbed' coaxial cylinder system, which will break down when the electric gradient (E_s) at the inner cylinder (along the plane of minimum airgap), reaches the critical breakdown gradient value – known for the corresponding unperturbed coaxial (and concentric) cylinder system, to occur in air at standard temperature and pressure conditions when $E = E_s = 27.2 + 13.35\sqrt{r}$, where r is the radius of the inner cylinder in centimetres. Predicted and experimental results agreed to within ± 5% for all sizes of inner conductor (radius r) considered.

Predicted and experimental sparking voltages have also been compared for numerous gaseous insulants, for a wide range of gas temperatures and pressures and for many different electrode systems, using simple perturbation field techniques. Excellent agreement has been demonstrated (e.g. see Table 3.4). For example, designers of GIS switchgear in the 1980s had access to a vast reliable database relating to the characteristics of numerous insulating materials and also SF_6 to assist them to achieve effective, competitive and reliable designs as a result of much dielectric research and development activities (see, for example, References 1, 13 and 21).

Table 3.4 Breakdown data for hemispherically ended rod/plate arrangement (r = 12.7 mm) [39]

	Gap g, mm	Breakdown voltage at relative density, kv		
		3	5	7
Experimental		100	158	210
Empirical*	20	102	158	214
Semi-empirical		103	162	220
Experimental		127	200	259
Empirical*	40	126	197	267
Semi-empirical		129	203	276
Experimental		144	227	288
Empirical*	80	143	222	301
Semi-empirical		142	227	310

* Estimate using eqn. 3.1, together with equation of form $rE = K_1pr + K_2$ derived from concentric sphere hemisphere data

3.5.2.2 Semi-empirical approach

As an alternative to the above empirical method, the author and his colleagues have investigated a so-called semi-empirical breakdown estimation method, based on streamer theory of gas breakdown [1]. For air, the criterion for minimum breakdown voltage was given by Pederson [44, 45] as

$$\ln \alpha_x + \int_o^x \alpha dx = \ln \alpha + \alpha x \tag{3.3}$$

where α_x is the numerical value of α, Townsend's first ionisation coefficient, at the head of the avalanche, of length x, at which the critical ion number is reached in an electron avalanche; in a nonuniform field, streamers are formed, resulting in corona or breakdown.

The left-hand side of eqn. 3.3 is evaluated from the electrostatic field distribution, obtained using a general field analysis program for practical arrangements or from precise equations for standard geometries [38,39]. The right-hand side of eqn. 3.3 is computed from existing empirical breakdown potential gradient data for uniform fields of gap x. The values of α used in both sides of eqn. 3.3 for the examples discussed in previous studies [38,39] have been published by earlier workers [1, 39].

This semi-empirical approach was extended to SF_6 using a modified form of eqn. 3.3, namely

$$\int_o^x (\alpha - \eta)\, dx = k = 18 \tag{3.4}$$

where α and η are Townsend's first ionisation coefficient and attachment coefficient, respectfully, in SF_6. An essential prerequisite of Pederson's

semi-empirical approach for any particular set of conditions is information concerning the following parameters:

(a) uniform field breakdown potential gradients
(b) α and η values
(c) potential-gradient distribution across the nonuniform gap.

General purpose digital computer programs have been developed which are capable of solving equations of the form of eqn. 3.3 to predict, with acceptable accuracy, the minimum breakdown voltage, V, for a wide range of standard and practical electrode arrangements in air, N_2 and SF_6, for pressures in the range 1–5 atmospheres [38,39,41] and for air at high temperatures.

Similarity and Paschen's law type relationships were also studied. For example, with uniform field gaps of 0.5–2.0 cm and temperatures 20–1100 °C, Powell and Ryan obtained results for the static breakdown of atmospheric air which fitted a relationship of the form

$$V_s = 24.49\,(\partial g) + 6.61/(\sqrt{\partial}\, g) \quad \text{(kV)} \quad \text{to within } +5\% \text{ and } -2\%$$

Here, the same constants were selected as given by Boyd *et al.* from their earlier study at standard atmospheric conditions, where the relative air density $\partial = 1.0$, $p = 1013$ mbar and $T = 293$ K (20 °C) (see eqn. 20.13, Chapter 20, and also eqn. 6.3, p. 540 [1]).

An example of these techniques is given in Table 3.4, which compares experimental and estimated breakdown voltages in air, at relative air densities (∂) of 3, 5 and 7, respectively, for a hemispherically ended rod/plate arrangement [radius $r = 12.7$ mm]. It is clearly seen that both these estimation methods are capable of predicting breakdown voltage levels to within ± 5% over the range of gaps and air pressures considered.

3.6 Summary

This chapter has provided a general introduction to the application of gaseous insulation systems. Although it has only been possible to touch very briefly on some major aspects, important strategic issues will be further developed in other chapters focusing on special areas. An indication has been given in this chapter of numerical field techniques which have found widespread application in the insulation design of GIS and other switchgear for many years. The simple breakdown estimation methods (empirical and semi-empirical) by Ryan *et al.*, which are extensions of the work by Schwaiger (1954) and Pederson (1967) [44,45] together with an available experimental database obtained from extensive Paschen's Law/similarity type studies in gaseous insulants, have been thoroughly developed to such a degree that minimum breakdown voltages of practical GIS design layouts (as well as a host of gas-gap

arrangements; see [1,5]) can be estimated to within a few per cent, at the design stage, often without recourse to expensive development testing. Such derived voltages are generally the minimal withstand levels attainable under practical conditions. Undoubtedly, there is still considerable scope in the future to predict dielectric performance by utilising advanced planning simulation tools incorporating genetic algorithms and artificial intelligence techniques, linked to various 'extensive databases' relating to breakdown characteristics of gaseous insulation, including equipment service performance data (e.g. from surveys similar to [33]).

Finally, it is anticipated that the continuing, and growing, environmental concerns will influence the development of the next generation of gas insulated switchgear but a commercial replacement for 100% SF_6 gas, for interruption purposes at the higher ratings, still seems remote!

3.7 Acknowledgments

The author wishes to thank the Directors of NEI Reyrolle Ltd (now VA TECH REYROLLE) for permission to publish earlier papers which have been extensively referred to in the studies reported in this chapter. He also gratefully acknowledges the assistance given by many of his former colleagues and for their contributions and generous support over the years.

3.8 References

1 BLAIR, D.T.A.: 'Breakdown voltage characteristics', *in* MEEK, J.M. and CRAGGS, J.D. (eds): 'Electrical breakdown of gases' (J. Wiley & Sons, 1978), Chap. 6, pp. 533–653
2 FLURSCHEIM, C.H. (ed.): 'Power circuit-breaker theory and design' (Peter Perigrinus Ltd., 1982)
3 RAETHER, H.: 'Electron avalanches and breakdown in gases' (Butterworth, 1964)
4 BRADWELL, A. (ed.): 'Electrical insulation' (Peter Perigrinus Ltd., 1983)
5 WATERS, R.T.: 'Spark breakdown in non uniform fields' in MEEK, J.M. and CRAGGS, J.D. (eds): 'Electrical breakdown of gases' (J. Wiley & Sons, 1978), pp. 385–532
6 LOOMS, J.S.T.: 'Insulators for high voltages' (Peter Perigrinus Ltd., 1990)
7 CIGRE Task Force 33.04.09 Report.: 'Influence of ice and snow on the flashover performance of outdoor insulators, Part I: Effects of ice', *Electra*, 1999, **187**, Dec., pp. 91–111
8 CIGRE Task Force 33.04.09 Report.: 'Influence of ice and snow on the flashover performance of outdoor insulators, Part II: Effects of snow', *Electra*, 2000, 188, Feb., pp. 55–69
9 LEGG, D.: 'High-voltage testing techniques'. Internal Reyrolle Research Report, 1970

10 RYAN, H.M. and WHISKARD, J.: 'Design and operation perspective of a British UHV laboratory', *IEE Proc. A*, 1986, **133**, (8), pp. 501–521
11 DIESENDORF, W.: 'Insulation co-ordination in high voltage electric power systems' (Butterworths, 1974)
12 IEEE Committee Report.: 'Sparkover characteristics of high voltage protective gaps', *IEEE Trans.*, 1974, **PAS-93**, pp. 196–205
13 RYAN, H.M., LIGHTLE, D. and MILNE, D.: 'Factors influencing dielectric performance of SF_6 insulated GIS', *IEEE Trans.*, 1985, **PAS-104**, (6), pp. 1527–1535
14 CIGRE Working Group 33.11, Task Force 03, SCHEI, A., Convenor WG33.11.: 'Application of metal metal oxide surge arresters to overhead lines', *Electra*, 1999, **186**, Oct., pp. 83–112
15 CIGRE Working Group 33.07 Report: 'Insulation coordination in live working and other special conditions in electrical system', Guidelines for insulation coordination in live working, *Electra*, 2000, **188**, Feb., pp. 139–143
16 MALIK, N.H. and QURESHI, A.H.: 'A review of electrical breakdown in mixtures of SF_6 and other gases', *IEEE Trans. Electr. Insul.*, 1979, **EI-14**, pp. 1–14
17 RYAN, H.M. and JONES, G.R.: 'SF_6 switchgear' (Peter Perigrinus Ltd., 1989)
18 JEFFERIES, D.: 'Transmission today: lessons from a decade of change', *Electra*, 1999, **187**, Dec., pp. 9–18. Reproduced opening speech: London CIGRE Symposium: Working plant and systems harder: Enhancing the management and performance of plant and power systems' 7–9 June 1999
19 URWIN, R.J.: 'Engineering challenges in a competitive electricity market'. Keynote address, ISH: High voltage symposium, 22–27 Aug. 1999, London, Paper 5.366.SO
20 ALI, S.M.G., RYAN, H.M., LIGHTLE, D., SHIMMIN, D., TAYLOR, S. and JONES, G.R.: 'High power short circuit studies on a commercial 420 kV, 60 kA puffer circuit-breaker', *IEEE Trans.*, 1985, **PAS-104**, (2), pp. 459–468
21 RYAN, H.M.: 'GIS barriers: application of field computation strategies to switchgear'. IEE Colloquim on *Field modelling: applications to high voltage power apparatus*, London, 17th Jan. 1996
22 RAGALLER, K.: 'Current interruption in high voltage networks' (Plenum Press, 1978)
23 MOSCH, W. and HAUSCHILD, W.: 'High voltage insulation with sulphur hexafluoride, VEB Verlag Technik Berlin, 1979
24 BOGGS, S.A., CHU, F.Y., HICK, M.A., RISHWORTH, A.B., TROLLIET, B. and VIGREUX, J.: 'Prospect of improving the reliability and maintainability of EHV gas insulated substations', CIGRE, 1982, Paper 23–10
25 RYAN, H.M. and WATSON, W.L.: 'Impulse breakdown characteristics in SF_6 for non-uniform field gaps', CIGRE, 1978, Paper 15–01
26 LAGHARI, J.R.: 'Review – A review of particle contaminated gas breakdown', *IEEE Trans. Electr. Insul.*, 1981, **EL-16**, p. 388
27 ISHIKAWA, M. and HATTIRI, T.: 'Voltage-time characteristics of particle initiated breakdown in SF_6 gas'. 3rd Int. Symp. On *Gaseous dielectrics*, Knoxville, USA, 1982, Paper No. 28

28 ETEIBA, M.G. and RIZK, A.M.: 'Voltage-time characteristics of particle-initiated impulse breakdown in SF_6 and SF_6–N_2', *IEEE Trans. Power Appar. Syst.*, 1983, **PAS-102**, (5), pp. 1352–1360
29 TAKUMA, T. *et al.*: 'Interfacial insulation characteristics in gas mixtures as alternative to SF_6 and application to power equipment', CIGRE, 2000, Paper 15–207
30 HAMPTON, B.F., PEARSON, J.S., JONES, C.J., IRWIN, T., WELCH, I.M. and PRYOR, B.M.: 'Experience and progress with UHF diagnostics in GIS'. CIGRE, 1992, Paper 15/23-03
31 JONES, C.J., HALL, W.B., JONES, C.J., FANG, M.T.C. and WISEALL, S.S.: 'Recent development in theoretical modelling and monitoring techniques for high voltage circuit-breakers'. CIGRE 1994, Paper 13–109
32 CIGRE Working Group 13.09.: 'Monitoring and diagnostic techniques for switching equipment', Convenor JONES, C.J., United Kingdom, *Electra*, 1999, **184**, June, p. 27
33 CIGRE Working Group 23.02, Task Force 02 Report.: 'Report on the second international survey on high voltage gas insulated substations(GIS) service experience', *Electra*, 2000, **188**, Feb., p. 127
34 GALLOWAY, R.H., RYAN, H.M. and SCOTT, M.F.: 'Calculation of electric fields by digital computer', *Proc. IEE*, 1967, **114**, (6), pp. 824–829
35 RYAN, H.M. and WALLEY, C.A.: 'Field auxiliary factors for simple electrode geometries', *Proc. IEE*, 1967, **114**, (10), pp. 1529–1534
36 MATTINGLEY, J.M. and RYAN, H.M.: 'Potential and potential-gradient for standard and practical electrode systems', *Proc. IEE*, 1971, **118**, (5), pp. 720–732
37 RYAN, H.M.: 'Prediction of electric fields and breakdown voltage levels for practical 3-dimensional field problems'. Eighth Universities Power Engineering Conference, 1973, University of Bath
38 BLACKETT, J., MATTINGLEY, J.M. and RYAN, H.M.: 'Breakdown voltage estimation in gases using semi-empirical concept'. IEE Conf. Publ. 70, 1970, pp. 293–297
39 MATTINGLEY, J.M. and RYAN, H.M.: 'Breakdown voltage estimation in air and nitrogen'. NRC Conference on Electrical and Dielectric Phenomena, 1971, Williamsburgh, USA, November
40 RYAN, H.M.: 'Prediction of alternating sparking voltages for a few simple electrode systems by means of a general discharge-law concept', *Proc. IEE*, 1967, **114**, (11), pp. 1815–1821; (6), pp. 830–831
41 SCOTT, M.F., MATTINGLEY, J.M. and RYAN, H.M.: 'Computation of electric fields: Recent developments and practical applications', *IEEE Trans. Electr. Insul.*, 1974, **EI-9**, (1), pp. 18–25
42 BINNS, D.F. and RANDALL, T.J.: 'Calculation of potential gradients for a dielectric slab placed between a sphere and a plane', *Proc. IEE*, 1967, **114**, (10), pp. 1521–28
43 STOREY, J.T. and BILLINGS, M.J.: 'Determination of the 3-dimensional electrostatic field of a curved bushing', *Proc. IEE*, 1969, **116**, (4), pp. 639–643
44 PEDERSON, A.: 'Calculation of spark breakdown or corona starting voltages in non-uniform fields', *IEEE Trans.*, 1967, **PAS-86**, pp. 200–206
45 PEDERSON, A.: 'Analysis of spark breakdown characteristics for sphere gaps', *IEEE Trans.*, 1967, **PAS-86**, pp. 975–978